RSC Advances

ROYAL SOCIETY OF CHEMISTRY

www.rsc.org/advances

Adsorption characterization of Pb (II) ions onto iodate doped chitosan composite: Equilibrium and kinetic studies

Asha H. Gedam[*a], Rajendra S. Dongre[b]

[*a] Department of Chemistry, Cummins College of Engineering for Women, Nagpur- 441110, India.
[b] Post Graduate Teaching Department of Chemistry, R.T.M. Nagpur University, Nagpur -440033, India.
E-mail: agedam.ccoew@gmail.com; Fax: 07104-280304, Mobile: (+91) 9730184638.

Abstract

Iodate doped chitosan (I-CS) composite was synthesized, characterized and used as an adsorbent for adsorption of Pb (II) ions from aqueous solution. The I-CS sorbent was extensively characterized by nitrogen adsorption/desorption to determine the BET surface areas and BJH pore size distribution, elemental analysis, TGA/DTA, FTIR, XRD and SEM. The influences of various chemical parameters viz. pH, contact time, dose of adsorbent and initial metal ion concentration on adsorption performance of Pb (II) ions were analyzed. Equilibrium adsorption isotherm and kinetics of adsorption has also been studied. The BET results exhibited decreased porosity and specific surface area of I-CS composite due to the blockage of internal porous cavities by incorporated iodate. The maximum removal of the Pb (II) ions using I-CS adsorbent was observed at optimum pH 6. The dose of adsorbent on the percentage removal of Pb (II) ions also has a prominent effect and maximum Pb (II) ions mitigation found at 0.5 g/L adsorbent dose with 99% efficiency achieved in 4h. The adsorption of Pb (II) ions shown applicability of the Langmuir and Freundlich adsorption isotherm suggests the existence of both heterogeneous surface and monolayer coverage of adsorbed molecules. The adsorption process follows pseudo-second-order kinetics. This doped composite adsorbent proved to be an effective for adsorption of Pb (II) ions from aqueous solution.

Keywords Iodate doped chitosan; Pb (II); Adsorption; Isotherm; Kinetics.

1. Introduction

The presence and high concentration of many heavy metals like lead, copper, zinc, mercury, chromium, arsenic and cadmium in various water resources can be injurious to the environment and public health. Among all the heavy metal ions, special attention has been given to Pb (II) ions contamination in water. Research on lead has become a prime importance for environmentalist and medical scientists because it has no biological use and highly fatal to human beings and aquatic flora and fauna even in relatively low concentration.[1] It affects the central nervous system, kidneys, liver, gastrointestinal system and it may directly or indirectly cause diseases such as anemia,

encephalopathy, hepatitis and the nephritic syndrome.[2] It is a cumulative poison and carcinogenic even at low concentration.[3] Levels of lead in drinking water, waste water and water used for agricultural and recreational purposes must be reduced to within the maximum allowable concentrations recommended by national and international health authorities such as World Health Organization (WHO). The Current EPA drinking water standard for lead are 0.05 mg/L but a level of 0.02 mg/L has been proposed and is under review. According to Indian Standard Institution (ISI) the tolerance limit for discharge of lead into drinking water is 0.05 mg/L and in land surface waters is 0.1mg/L.[4] The wide usage of Pb (II) in various industries has triggered the necessities of developing an efficient method to remove this heavy metal ion from wastewaters. Many conventional methods are known for lead removal from water namely chemical precipitation, membrane separation, ion exchange**,** coagulation, reverse osmosis, evaporation and adsorption. The adsorption process is found to be effective and economic for wide variety of water pollutant sorption.[5]

Several studies are reported for the removal of heavy metal ions from water. Biosorption of Lead (II) from aqueous solutions by non-living algal biomass has been reported.[6] An expensive and effective adsorbent from bagasse fly ash obtained from a sugar industry has been developed for the removal of lead and chromium.[7] Red mud from aluminum industry has been converted into an inexpensive and efficient adsorbent and the authors have used this adsorbent for the removal of lead and chromium from aqueous solution.[4] studies conducted on the kinetic parameter for the removal of lead and chromium from wastewater using activated carbon developed from fertilizer waste material.[8] Recently, adsorptions using biomaterials has been considered as one of the most favorable option in treating wastewater as they are adequate, biodegradable, ecofriendly, non-toxic and have the capability to physically or chemically interact with a variety of molecules.[9] A natural nitrogenous polysaccharide material chitosan that can be obtained in large amounts and cheap used in wastewater treatment. Chitosan is obtained by the N-deacetylation of chitin using an alkaline solution. It is a heterogeneous cationic polymer composed of 2-amino-2-deoxy-D-glucopyranose and residual 2-acetamido-2-deoxy-D-glucopyranose.[10] Chitin and chitosan are of commercial importance because of their high nitrogen content (6.89%) and their excellent properties such as biocompatibility, biodegradability, non-toxicity and adsorptive abilities. Chitosan has the ability to form complexes with metals. It has a better adsorption capacity for metal ion. It has severe limitations in its use in acidic media because of its solubility in acid.[11] Chitosan shows high affinity for metal ions adsorption due to the presence of amine ($–NH_2$) and hydroxyl (–OH) functional groups acts as chelating sites. The deacetylated amino groups in chitosan can be chemically modified easily.[12] Therefore the certain functional groups are also expected to have an adsorptive impact on heavy metals ions. Various chitosan based adsorbents such as magnetic chitosan/graphene oxide material,[13] graphite doped chitosan composite,[14] chitosan tripolyphosphate,[15] bromine pretreated chitosan,[16] for lead (II) ions removal has been reported. chitosan immobilized on silica for removal of Zn(II), Cu(II), Cd(II), Pb(II), Fe(III) V(V), Mo(VI) has been investigated.[17] Support materials for chitosan that have been

previously studied are sand for Cu(II) and Pb(II) removal,[18] Chitosan - bentonite for Cu(II), Ni(II) and Pb(II) removal.[19] Adsorption of Hg^0 from coal combustion flue gases by novel iodine-modified bentonite/chitosan sorbents.[20] Removal of elemental mercury by iodine-modified rice husk ash sorbents was reported.[21] Adsorption Properties of Iodine-doped pitch-based activated carbon fiber,[22] Hg^0 capture by halogenated activated carbon, such as chlorine impregnation,[23] iodine impregnation, carbon-based and noncarbon sorbents modified by iodine [24] have been studied for the improved mercury removal after modification.

To the best of our knowledge, there is no literature reported on the removal of Pb (II) ions from water using iodate doped chitosan (I-CS) composite. Due to this reason, the present study attempt to find out whether the new surface chemistry of chitosan modified by iodate salt have an impact on Pb(II) removal. This gave way for more adsorption studies for Pb (II) ions to be conducted using I-CS. In present study, I-CS sorbent was synthesized and the properties of adsorbent are investigated through SEM, XRD, TGA/DTA, BET, and FTIR analyses. The effect of contact time, adsorbent dosage, pH and initial metal ion concentration on Pb (II) removal using I-CS were systematically studied. The Langmuir and Freundlich isotherms were used to evaluate the equilibrium adsorption data. The kinetics of adsorption was determined based on the pseudo first order, Pseudo second order and intraparticle diffusion models.

2. Materials and methods

Chitosan used as an adsorbent was purchased from Sisco Research Laboratories, Mumbai (India), Potassium iodate (Merck, India) anhydrous ethanol (Merck, India). All chemicals used were of analytical reagent grade. Lead (II) nitrate (Merck, India) was used for preparation of standard 1000 mg/L Pb (II) ion solution. The required working standards of Pb (II) solutions were prepared from standard lead nitrate solution by successive dilution using double distilled water. Acetic acid (Merck, India) and ammonium hydroxide (Merck, India) used without further purification. The pH of the medium was adjusted using 0.1 N nitric acid (Fisher scientific, India) and 0.1 N sodium hydroxide (Merck, India).

2.1 Preparation of I-CS composite

Chitosan (Mw = 200,000 Da, degree of deacetylation > 90 %) dissolved in 3% acetic acid heated at 40-50°C to obtain homogeneous gel. Potassium iodate treated with anhydrous ethanol was added to chitosan gel in (1:1 w/w) under a vigorous mechanical stirring. Then mixture was magnetically stirred (800 rpm) at room temperature (27 °C) for 5-6 hours. This mixture was dropped in 50% aqueous ammonia. Finally it was filtered, washed several times with distilled water and dried in oven at 80 °C. The adsorbent was grounded, sieved to 150 mesh sizes and stored into the sorbent bottle for further adsorption study.

2.2 Characterizations

Brunauer-Emmet-Teller (BET) surface area of the sample was determined by nitrogen adsorption-desorption method at 77 K using Micromeritics ASAP 2020 V3.04 H analyzer (USA). Elemental analysis was used to estimate the density of the active sites in the sorbent. Carbon, hydrogen, nitrogen, and sulfur wt % (absolute weight) were performed by an elemental analyzer (EL cube, Vario Inc., Germany). The thermal stability of the sample was evaluated using thermal gravimetric analysis (TGA/DTA) (Perkin Elmer Diamond instrument). Fourier Transform Infrared (FTIR) Spectroscopy were recorded in the range of 450-4000 cm^{-1} to study the functional groups and surface chemistry of the adsorbent (Perkin Elmer spectrum one, Germany) using the KBr pressed pellet technique. XRD measurements were taken with Rigaku MiniFlex2 Goniometer using Cu Kα radiation as X-ray source. The surface morphology of chitosan and I-CS composite was studied by using scanning electron microscope (SEM) at an accelerating voltage of 15kV using (Zeiss Sigma, Germany).

2.3 Batch adsorption experiments

Batch mode adsorption experiments were carried out with 0.05 g of adsorbent at room temperature (27°C) with 100 ml of required Pb (II) ions solution in 250 ml Erlenmeyer flasks agitated on rotary shaker at 200 rpm. Adsorption isotherm studies were carried out by varying Pb (II) ion concentration from 35 to 115 mg/L at optimum pH 6. pH alterations were done using 0.1 N HNO_3 or 0.1 N NaOH. All the flasks were agitated at 200 rpm at room temperature for 280 minutes to reach adsorption equilibrium. The reaction mixture was filtered through Whatman filter paper-41 and analyzed for residual Pb (II) ions concentration by atomic absorption spectrophotometer (SensAA GBC scientific equipment). In adsorption kinetic experiments the samples were agitated and withdrawn at interval of 20 to 280 min to determine metal ion concentration. The percentage removal of Pb (II) was calculated using equation (1)

$$\% \text{ removal} = \frac{C_i - C_f}{C_i} \; x \; 100 \qquad (1)$$

Adsorption capacities were calculated using equation (2) and (3) respectively.

$$q_e = \frac{C_i - C_f}{m} \; x \; V \qquad (2)$$

$$q_t = \frac{C_i - C_t}{m} \; x \; V \qquad (3)$$

Where q_e and q_t were the amounts of metal ions adsorbed at equilibrium and at time t respectively in (mg/g). C_i and C_f were the initial and final Pb (II) ions concentration in (mg/L). C_t was the residual metal ion concentration at time t in (mg/L). V is the volume of solution (L) and m represents mass of adsorbent (g).

2.4 Desorption experiment

The desorption study was carried out with 35 mg/L, 75 mg/L and 115 mg/L Pb (II) ion concentration. 0.05 g of lead loaded I-CS adsorbent was washed with distilled water, air dried and placed in contact with 0.1M HCl as desorption agent in 250 ml Erlenmeyer flasks. Desorption experiments were carried out at pH 3. The flasks were agitated at 200 rpm at 27 °C for 10 hrs to ensure the equilibrium. To estimate the process of Pb (II) desorption, the Pb (II) ion concentration present in 0.1 M HCl were analyzed using Atomic absorption spectrophotometer. The percentage desorption of Pb (II) was calculated using equation (4).

$$\% \text{ desorption} = \frac{C_A - C_D}{C_A} \text{ X } 100 \qquad (4)$$

Where C_A and C_D are the concentration of Pb (II) ions adsorbed and desorbed (mg/L) respectively. The adsorbent was reused in four adsorption-desorption cycle.

3 Results and discussion

3.1 Physicochemical characterization of I-CS composite

3.1.1 BET and Elemental Analysis

The elemental analysis such as (C, H, N, and S) of CS and I-CS sorbents is given in table 1. BET surface areas and pore structures of CS and I-CS adsorbents are also provided in Table 1. It was found that the iodate doping actually decreased the BET surface areas and the pore volumes of I-CS composite due to the blockage of internal porosity by incorporated KIO_3. Since the average pore size of the sample also increased after modification, the blocked pores would be micropores, resulting in a decrease of specific surface area and total pore volume.[25] Fig. 1 (A) shows the nitrogen adsorption-desorption isotherm of CS and I-CS composite. They exhibit typical Type IV isotherm according to IUPAC classification which corresponds to the presence of large amount of mesopores and/or macropores. The hysteresis exists due to the presence of slit shaped pores. The BJH based pore size distributions of CS and I-CS are also shown in Fig. 1(B). The peaks in the range of 2 to 6 nm for I-CS composite are located in the mesopore ranges. The adsorption capacity of adsorbent increases with increasing surface area for pure physisorption process.[26] It was observed that the BET surface area of I-CS adsorbent was smaller than pure chitosan. Therefore it is concluded that the physisorption of I-CS for Pb(II) ions is limited and the chemisorptions is the predominant adsorptive mechanism due to presence of active binding sites for the Pb(II) ions.

Table 1 Pore Structure Parameters and Elemental Analysis of CS and I-CS Sorbents.

Sorbents	BET (m^2/g)	V_{total} (cc/g)	V_{micro} (cc/g)	V_{meso} (cc/g)	Mean pore diameter (nm)	Element (wt %)				
						C	H	N	S	O
CS	3.5	4.582	0.004	4.578	5.23	38.51	7.8	7.05	0.19	46.45
I-CS	0.87	2.126	0.0118	2.1142	9.77	37.17	7.14	7.01	0.18	48.5

Where V_{total}: total pore volume, V_{micro}: micropore volume, V_{meso}: mesopore volume of CS and I-CS composite.

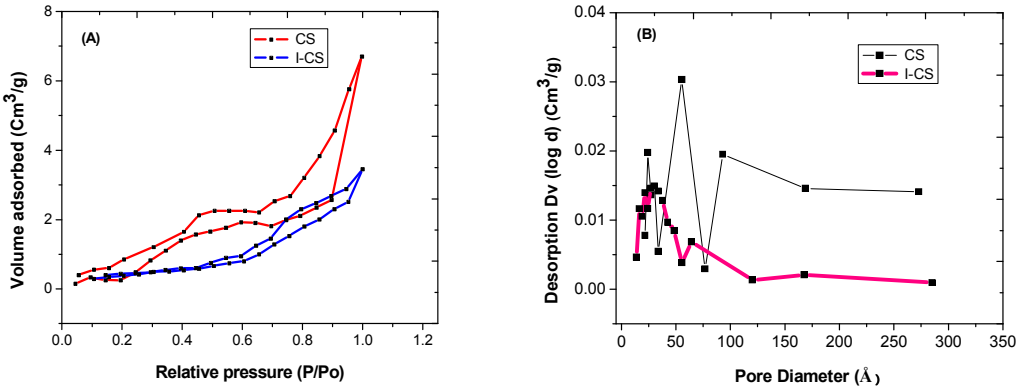

Fig. 1 (A) Nitrogen adsorption-desorption isotherm (B) BJH based pore size distribution of CS and I-CS composite.

3.1.2 FTIR spectra analysis

FTIR spectra of pure chitosan, I-CS composite before and after Pb (II) ions adsorption are presented in Fig. 2. The Peaks of chitosan at 3073 cm^{-1} and 2876 cm^{-1} are assigned to the hydroxyl groups.[27] The peaks at 1667 cm^{-1} for carbonyl C=O stretch in amide, 1530 cm^{-1} due -NH bending in amide.[28] The broad peak at 1077 cm^{-1} assigned to C-O stretching of the ring C-O-H, C-O-C and CH_2OH.[29] The absorption peak at 990 cm^{-1} corresponds to saccharide structure.

In I-CS composite the wide absorption band at 3073 cm^{-1} was shifted to the higher wavenumber at 3264 cm^{-1}, corresponding to the stretching vibration of $-NH_2$ and -OH groups. Similarly the absorption peak at 1530 cm^{-1} for N-H bending in amide was shifted to higher wavenumber at 1554 cm^{-1}. This is due to the fact that physical blend and chemical interaction of two or more polymers illustrate the changes in characteristics absorption peaks.[30] The significant changes of N-H stretching and N-H bending after modification of chitosan indicate that the N-H vibration is affected due to the modification.[31] In I-CS composite new absorption bands at 2946 cm^{-1} for CH_3 asymmetric stretching, 2840 cm^{-1} for CH_2 symmetric stretching and 2147 cm^{-1} for C-N stretching vibrations appeared. Similarly new absorption bands at 830 cm^{-1} and 808 cm^{-1} in the region of 515-830 cm^{-1} indicating the presence of iodate compounds.[32-35] The appearance of new absorption peaks in I-CS suggested the interaction between iodate and chitosan to form a composite.

The spectral investigation of I-CS adsorbent after Pb (II) adsorption showed that the peaks either decreases in intensity or disappear might involve in metals adsorption.[36, 37] The peaks at 3264 cm^{-1}, 2840 cm^{-1}, 2147 cm^{-1}, 1664 cm^{-1}, 899 cm^{-1}, 830 cm^{-1} and 808 cm^{-1} lost after lead adsorption, indicated the participation of –OH, C-N, C=O and iodate groups in forming complexes with Pb (II) ions. The FTIR spectrum of lead-loaded I-CS composite shows some shift in wavenumbers. The band at 1554 cm^{-1} and 1071 cm^{-1} shifted to 1506 cm^{-1} and 1067cm^{-1} respectively suggested the involvement of N-H and C=O group in Pb(II) adsorption.[38] The FTIR analysis revealed the functional groups –OH, C-N, C=O, iodate and NH_2 responsible for Pb(II) adsorption on I-CS composite.

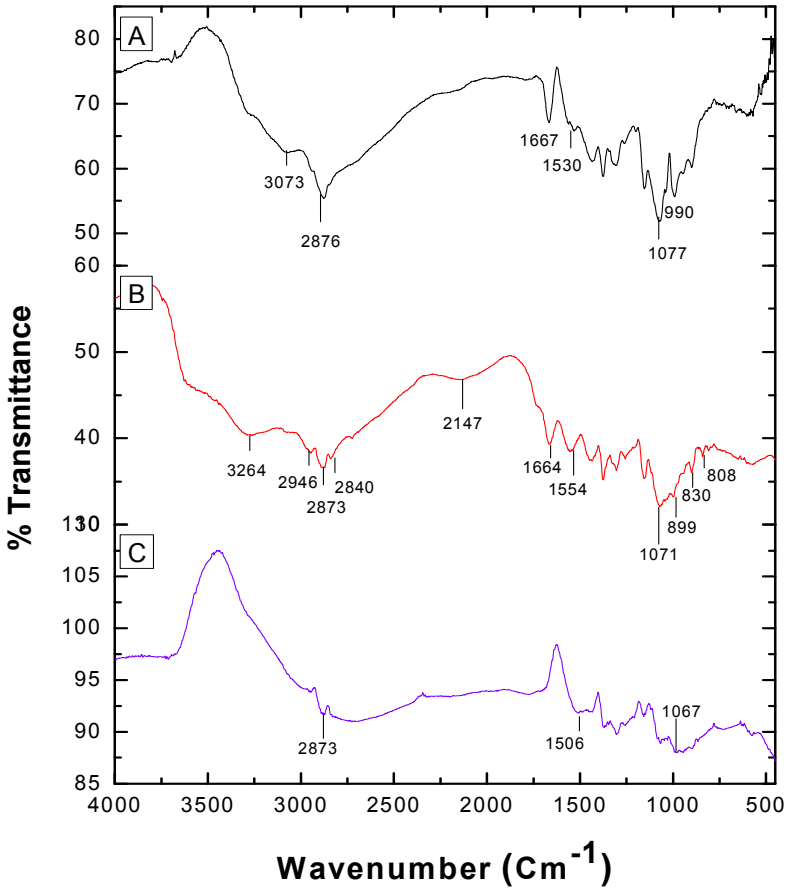

Fig. 2 FTIR spectra of (A) pure chitosan, (B) I-CS composite before Pb(II) adsorption and (C) I-CS composite after Pb(II) adsorption.

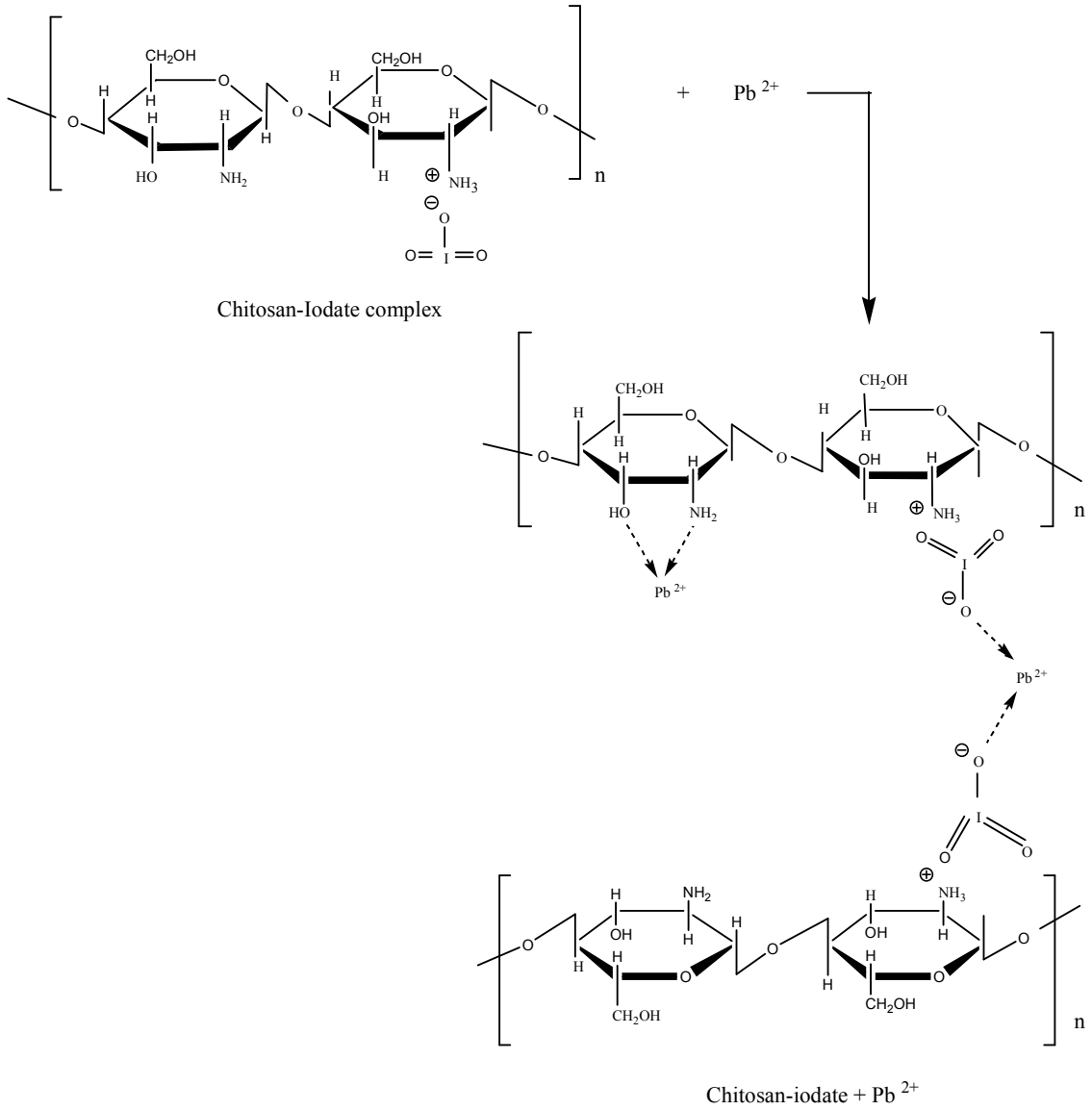

Fig. 3 Binding mechanism for the Pb (II) ions adsorption onto I-CS composite.

3.1.3 X-ray diffraction analysis

XRD patterns of pure chitosan, I-CS composite before and after Pb (II) adsorption are shown in Fig. 4 (A), (B) and (C) respectively. X-ray diffraction pattern of chitosan exhibited broad diffraction peak at $2\theta = 20°$ with d- spacing of 4.2 Å is characteristics of semi crystalline chitosan. [39] In I-CS composite , the XRD pattern is slightly broadened and shown a small hump at $2\theta = 25°$ and at $2\theta = 34°$ as compared to pure chitosan indicating amorphous nature of synthesized composite. The XRD pattern of I-CS composite after Pb (II) adsorption shows some additional crystalline peaks related to Pb (II) adsorption. The XRD studies revealed the blending between iodate and chitosan and adsorption of Pb (II) ions on I-CS composite.

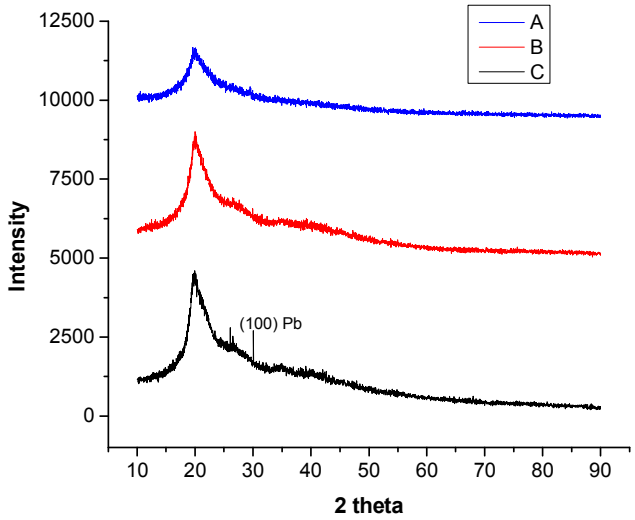

Fig. 4 XRD pattern of (A) pure chitosan (B) I-CS composite before Pb (II) adsorption (C) I-CS composite after Pb (II) adsorption.

3.1.4 Thermo gravimetric analysis

Thermo gravimetric analysis / Differential Scanning Calorimetry (TGA/DSC) was used to evaluate the thermal stability and to determine the decomposition temperature of pure chitosan and I-CS composite. TGA/DSC analysis of pure chitosan and I-CS composite is shown in Fig. 5 (A) and (B) respectively. The TGA of pure chitosan showed two steps of degradation, initial degradation occurred at around 30-100°C with 5 % weight loss which may correspond to a loss of adsorbed/bound water/ moisture vaporization.[40] Initial decomposition around 100 °C for pure chitosan can be attributed to the strong water adsorptive nature of chitosan. The second stage of degradation occurred at 270.97 °C and continued up to 312.18 °C. There was 46.28 % weight loss occurring in the second stage due to degradation of pure chitosan biopolymer and the temperature at which maximum degradation observed was 288.35 °C. At the end of 955.1 °C the total weight loss of sample was 70 %.

The TGA of I-CS composite exhibited two steps of degradation and first stage decomposition occurred between 30 °C until 200 °C which showed about 10 % weight loss due to evaporation of water. The second stage of decomposition of I-CS composite showed a weight loss of 30.88 % in temperature range of 259.50 °C to 304.03 °C. The maximum degradation occurred at temperature 280.26 °C. Two exothermic peaks were observed in DSC at different temperature ranges. The first peak corresponding to physically adsorbed water in the temperature range of 140-170 °C.[12] The second peak exhibited a rapid weight loss at 260-300 °C reaching a maximum at 283 °C for I-CS composite and 292 °C for pure chitosan. The second degradation stage of I-CS composite sorbent took place at lower temperature than the corresponding stage of pure chitosan indicating that I-CS

composite is less stable than pure chitosan due to the weakening of inter and extramolecular hydrogen bonding [41] and the presence of some active sites for Pb(II) removal.

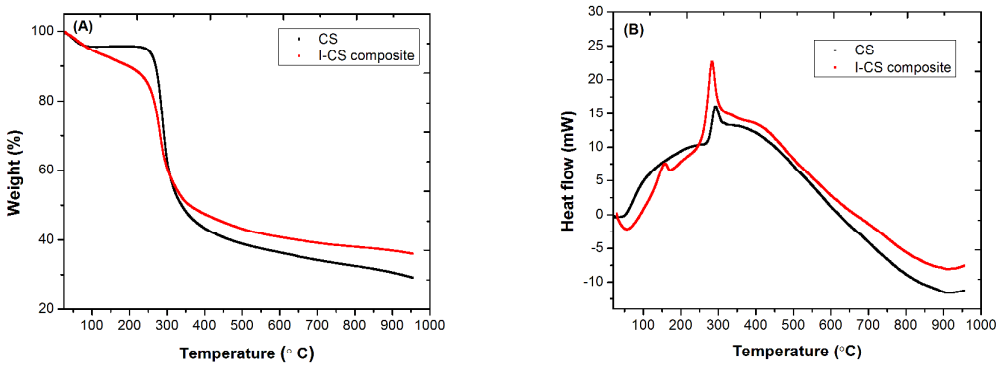

Fig. 5 (A) TGA (B) DSC of Pure chitosan and I-CS composite.

3.1.5 Scanning electron microscope (SEM) analysis

In order to confirm the adsorption of metal ions on I-CS composite and for more information concerning the alteration of the surface morphology after Pb (II) adsorption, a microscopic SEM technique was applied. The SEM images of pure chitosan, I-CS adsorbent before and after Pb (II) adsorption are given in Fig. 6 (a), (b) and (c) respectively. Fig. 6 (a) represented the surface morphology of chitosan with uneven texture, bumpiness and porous cavities. Fig. 6 (b) indicated the different surface morphology of I-CS adsorbent than with pure chitosan. In I-CS composite the bumpiness was lost after doping of iodate with chitosan. Similarly the adsorbent surface was highly irregular and porous in nature with large number of round or elliptical shape cavities. This will provide the surface for adsorption of Pb (II) ions. Fig. 6 (c) shows the complete change of surface morphology of adsorbent after Pb (II) adsorption where the porous structure is quite shallow and not clearly be seen. Pb (II) ions cover the surrounding adsorbent particles and filled the voids. The SEM of exhausted adsorbent clearly indicated coverage of the surface of the adsorbent due to adsorption of metal ions, presumably leading to formation of a monolayer of the metal ion over the adsorbent surface.

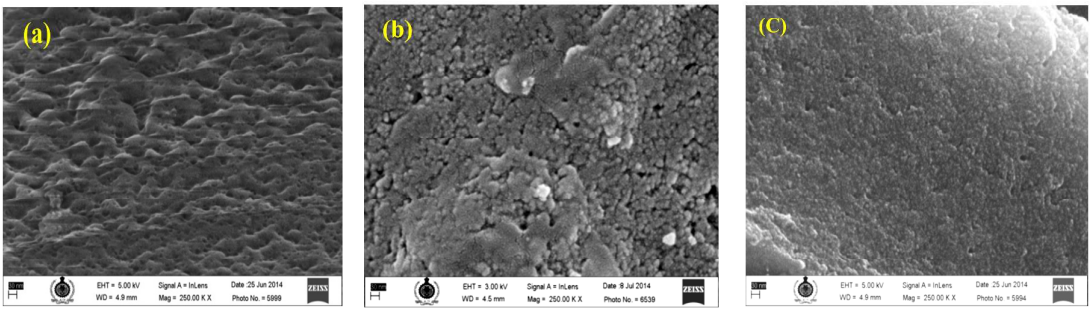

Fig. 6 SEM images of (a) Pure chitosan (b) I-CS composite before Pb(II) adsorption (C) I-CS composite after Pb(II) adsorption.

3.1.6 Point zero charge

In order to understand the adsorption mechanism, it is necessary to determine the zero charge point (pH_{PZC}) of the adsorbent.[42] Point of zero charge is of prime importance in the field of environmental science. It determines how easily an adsorbent adsorbs toxic ions. Cationic adsorption is favored at pH > pH_{PZC} and anionic adsorption is favored at pH < pH_{PZC}.[11] The pH at point zero charge (pH_{PZC}) of the I-CS adsorbent was determined by solid addition method.[43] 50 mL KNO_3 was transferred to a series of 100 ml conical flasks. The initial pH (pH_i) of these solutions was roughly adjusted from 2 to 10 using either 0.1 N HNO_3 or 0.1 N NaOH solutions. The pH_i of the solution was accurately noted followed by addition of 0.1 g of I-CS to each flasks. The flasks were allowed to equilibrate for 24 h with intermittent manual shaking. The final pH (pH_f) values of the supernatant liquids were noted. The difference between pH_i and pH_f values was plotted against pH_i . The point of intersection of the resulting curve at which difference between pH = 0 noted as $pH_{PZC.}$ Finally the point of zero-charge, as shown in Fig. 7 (A) was evaluated to be 3.9. This indicates that the adsorbent was acidic in nature and acquires a positive charge below pH 3.9. Thus, the adsorption of cations in case of heavy metals is favored at pH values above the $pH_{PZC.}$[44]

3.2 Effect of pH

To ascertain the effect of pH on the adsorption of Pb (II) ions, the batch equilibrium experiments were carried out at different pH values of 3-8 as shown in Fig. 7 (B). The experiments were performed for an initial concentration of 35 mg/L with 0.5 g/L adsorbent dose at room temperature (27 °C). It was observed that the percentage removal of Pb (II) increased with increase in the pH from 3 to 6. The maximum 95 % Pb (II) removal occurred at pH 6, after which there is regular decrease in the percentage removal with increase in pH up to 8. In general, at low pH values (pH < pH_{PZC}) the H^+ ion concentration far exceeds that of the Pb (II) ions and hence H^+ ions compete with metal ions for the adsorption sites followed by decreased Pb(II) ions adsorption capacity. By increasing the pH (pH > pH_{PZC}), the negative charge density on the adsorbent surface increasing and consequently the reduced amount of protons in the solution weakens the competition with Pb (II) for binding sites. This results in a higher adsorption amount of Pb (II) by the electrostatic interaction. The fundamental mechanism that governs the adsorption of Pb (II) ions by I-CS composite at pH < pH_{PZC} is adsorption and at pH > pH_{PZC} is adsorption and ion exchange. The decrease adsorption of Pb (II) above pH 6 was probably due to the precipitation of Pb (II) ions as lead hydroxides but not due to adsorption. [45-48] Thus adsorption process is a combination of ion exchange and precipitation. In this study, the optimum pH for Pb (II) removal was found 6.0 and further adsorption experiments were performed at this pH value.

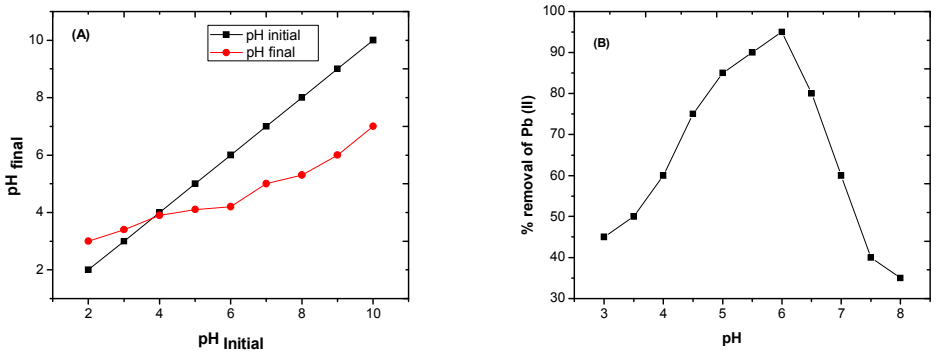

Fig. 7 (A) Point zero charge of I-CS composite (B) Percentage removal of Pb(II) at various pH ranges.

3.3 Effect of contact time on Pb (II) adsorption

The effect of contact time on Pb (II) removal is shown in Fig. 8. The batch studies were carried out at room temperature (27 °C) with varying initial metal ion concentration from 35 mg/L to 115 mg/L using 0.05 g of adsorbent dosage at pH 6. The result shows that the percentage of Pb (II) removal increases with increasing contact time from 20 min to 240 min. From 240 to 280 min, the percentage removal of Pb (II) remains constant due to the attainment of equilibrium, indicating that 240 min of contact time is enough for the maximum removal of Pb (II) ions from aqueous solution. Equilibrium adsorption achieved may be due to the accumulation of Pb (II) ions on the vacant sites causes limited mass transfer of the adsorbate from the bulk liquid to the external surface of adsorbent.[49] Equilibrium time is of crucial importance as it is one of the parameter for economical wastewater treatment plant application. From Fig. it is clear that, Pb (II) removal was highly concentration dependent. In fact the adsorption increases for higher metal ion concentration. The result exhibited that at a fixed dose of adsorbent the amount of Pb (II) ions adsorbed increases with increasing solution concentration but the percentage of adsorption decreased. It may be explained on the basis that at low Pb (II)/adsorbent ratio the active binding sites of adsorbent remains unsaturated offering large surface area for metal ion adsorption while at higher Pb (II)/adsorbent ratio, exchangeable adsorption sites are saturated, resulting in a decreased efficiency of Pb (II) ion adsorption.[50]

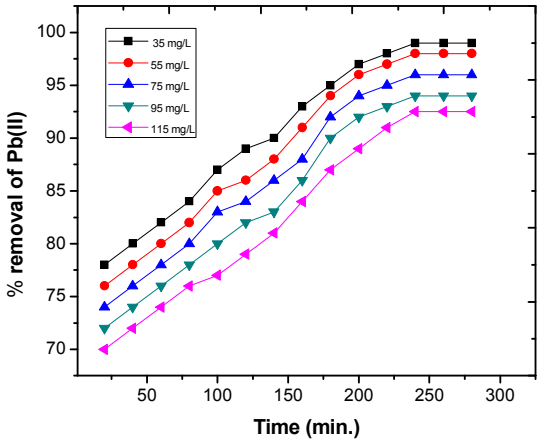

Fig. 8 Effect of contact time on Pb (II) ions removal at various initial concentrations.

3.4 Effect of adsorbent dose

The effect of adsorbent dose at constant temperature 27 °C and at optimum pH 6 on the percentage removal of Pb (II) is shown in Fig. 9. It can be seen that the removal extent of Pb (II) increases as the amount of adsorbent increases from 0.1 to 0.5 g/L with adsorption capacity of 81 % to 98 %. When the adsorbent dose increases, the number of adsorption sites on the adsorbent surface increases which results in maximum Pb (II) removal from the solution.[51] Beyond 0.5 g dose of adsorbent the Pb (II) removal efficiency is negligible due to attainment of equilibrium. These results clearly indicated that the optimum adsorbent dose must be fixed at 0.5 g/L and is justified for cost-effective purpose that leads to constant Pb (II) removal.

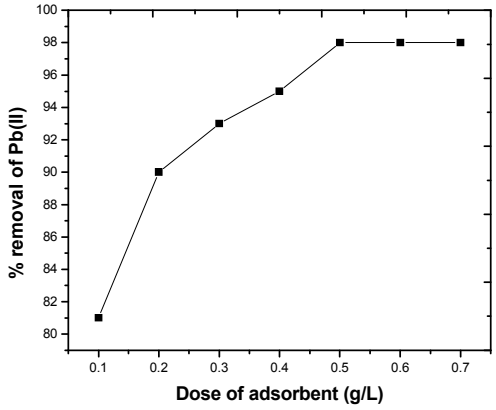

Fig. 9 Percentage removal of Pb (II) ions at various adsorbent doses.

3.5 Regeneration Studies

The percentage desorption of Pb (II) ions as depicted in Fig. 10. In present work, four adsorption-desorption cycles were performed using the desorbing agent 0.1 M HCl. The result revealed that the % desorption increases as the initial metal ion concentration increases. It is obvious that the detachment of Pb (II) ions from I-CS surface is directly proportional to the sites occupied by the adsorbed metal ions. It was found that as the initial metal ion concentration increases from 35, 75 and 115 mg/L, the more metals ions are adsorbed resulting in higher rate of desorption at 115 mg/L. The percentage recovery of metal ions decreased by 25-30% at the end of fourth adsorption desorption cycle due to saturation of adsorbent binding sites. 0.1 M HCl found to be better desorbing agent at pH 3 due to high amount of H^+ ions in the solution. This results in exchange of ions where H^+ takes the place of Pb (II) ions in solution. Consequently under acidic condition, the dissolution of adsorbent occurred releasing the large amount of Pb (II) ions bound onto I-CS into the solution.

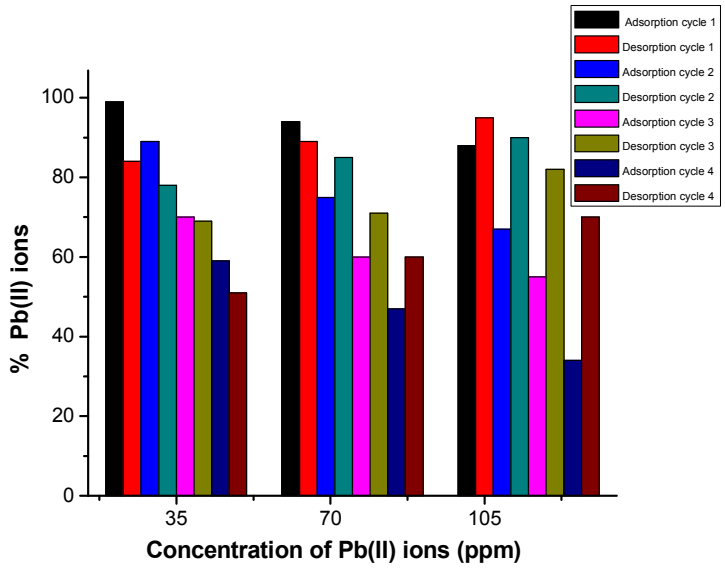

Fig. 10 Adsorption-Desorption cycles of different Pb (II) ions concentration onto I-CS composite.

3.6 Adsorption isotherm models

Many sorption isotherm models are used to determine the adsorption isotherm data and to predict the maximum adsorption capacity of the adsorbent. The experimental data were fitted into the most widely used Langmuir and Freundlich isotherm models. The Langmuir model assumes monolayer adsorption onto the surface of adsorbent containing a finite number of identical sites.[52] The Langmuir equation can be expressed as follows

$$\frac{C_e}{q_e} = \frac{1}{Q_o b} + \frac{C_e}{Q_o} \qquad (5)$$

Where C_e (mg/L) is equilibrium concentration of Pb (II) in solution, q_e (mg/g) is the amount of Pb (II) adsorbed per unit weight of adsorbent at equilibrium. Q_0 (mg/g) is the maximum adsorption amount. b (L/mg) is the Langmuir constant representing energy of adsorption. Q_0 and b obtained from slope and intercept of the plot of C_e/q_e against C_e as shown in Fig. 11. Favorability of adsorption of Pb (II) on I-CS was tested during the essential feature of the Langmuir isotherm expressed in terms of a dimensionless constant, R_L (separation factor) which can be expressed as $1/ (1+b.C_0)$.[53] The value of R_L indicated the type of Langmuir isotherm to be $R_L>1$ Unfavorable isotherm, $R_L=1$ Linear isotherm, $R_L=0$ Irreversible isotherm and $0<R_L<1$ Favorable isotherm. The value of R_L in many adsorption systems in range of 0 to 1 indicates favorable adsorption.

Freundlich isotherm model is useful in multilayer adsorption system. It is an empirical equation employed to describe that metal ions adsorption takes place on a heterogeneous adsorbent surface.[54] Freundlich isotherm model for sorption of Pb (II) on I-CS composite as shown in Fig. 11. The logarithmic form of Freundlich adsorption isotherm is represented as follows

$$\text{Log } q_e = \text{Log } K_F + \frac{1}{n \log C_e} \qquad (6)$$

Where K_F and n are Freundlich isotherm constants indicating adsorption capacity and adsorption intensity respectively. The Freundlich constant i.e. 1/n and K_F were calculated from the slope and intercept of Freundlich plots of log q_e versus log C_e. The parameter 1/n is related to the degree of surface heterogeneity. A smaller 1/n value indicates more heterogeneous surface whereas a value closer to or even one indicates the adsorbent has relatively more homogeneous binding sites.[55] The correlation coefficient and the other parameters obtained from Langmuir and Freundlich adsorption isotherm for sorption of Pb (II) ions are shown in Table 2.

Estimates of the Langmuir parameters with correlation coefficient R^2 =0.99 and the Langmuir constant b=0.314, showed a good applicability of this model. Similarly the value of R_L for the adsorption onto I-CS composite was in the range of 0.083-0.026 for 35 mg/L to 115 mg/L Pb(II) concentration and this specifies effective adsorption under the optimized experimental conditions.

The adsorption of Pb(II) ions by I-CS composite can also be explained by the Freundlich model with correlation coefficient R^2 = 0.98. The Value of 1/n obtained for Pb (II) ions was 0.355 indicating the heterogeneous adsorption binding sites of the adsorbent. The Langmuir and the Freundlich models both could be used to describe the adsorption data well, showing the fact that both monolayer and heterogeneous surface conditions exist under the experimental condition used. It signifies the complex and more than one adsorption mechanism of Pb (II) ions onto I-CS composite. It is well known that the Langmuir isotherm corresponds to a dominant ion exchange mechanism while the Freundlich isotherm shows adsorption-complexation reactions taking place in the adsorption process.[56]

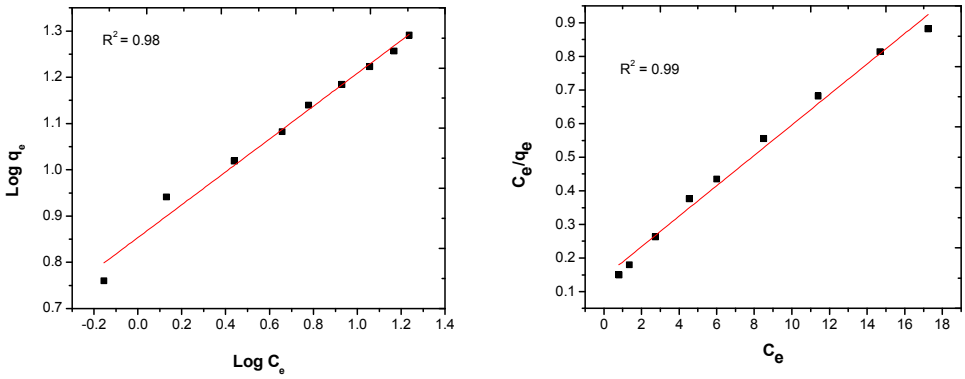

Fig. 11 Plot of Log C_e versus Log q_e Freundlich adsorption isotherm and Plot of C_e versus C_e/q_e Langmuir adsorption isotherm.

Table 2 Langmuir and Freundlich parameters for the adsorption of Pb (II) ions on I-CS composite

Equilibrium model	**Langmuir isotherm model**				**Freundlich isotherm model**		
Parameter	Q max (mg/g)	b (L/mg)	R^2	R_L	K_F (mg/g)	1/n	R^2
Value	22.22	0.314	0.99	0.083-0.026	7.12	0.355	0.98

3.7 Adsorption kinetics

The kinetic parameter used to govern the rate of adsorption and provides important information for designing and modeling the process. The adsorption kinetics is commonly modeled with the pseudo first order [57] and pseudo second order.[58]

Rate equation for the pseudo first order is generally expressed as follows

$$\frac{Dq_t}{dt} = K_1 (q_e - q_t) \qquad (7)$$

Where q_e and q_t are the sorption capacities at equilibrium and at time t, respectively (mg/g) and K_1 is the rate constant of pseudo first order sorption (min^{-1}). After integration and applying boundary conditions, $q_t = 0$ to $q_t = q_t$ at $t = 0$ to $t=t$, the integrated form of equation (7) is expressed as below

$$\text{Log } (q_e - q_t) = \text{Log } q_e - \frac{K_1}{2.303\ t} \qquad (8)$$

Fig. 12 shows the Langergren pseudo first order kinetic plot for the adsorption of Pb (II) ions onto I-CS composite. The pseudo first order rate constant can be obtained from the slope of plot between Log (q_e-q_t) against time t.

Ho presented a pseudo second order rate law expression, which demonstrated how the rate depended on the adsorption equilibrium capacity but not the concentration of the adsorbate.[59] The pseudo second order rate expression is as follows

$$\frac{dq_t}{dt} = K_2 (q_e - q_t)^2 \qquad (9)$$

Where q_e (mg/g) and q_t (mg/g) are the sorption capacity of Pb (II) at equilibrium and at time t respectively. K_2 is the pseudo second order rate constant (g/mg^{-1}min^{-1}). For the boundary conditions q_t = 0 to q_t=q_t at t=0 to t=t the integrated linear form of equation is as follows

$$\frac{t}{qt} = \frac{1}{K_2 qe^2} + \frac{1}{q_e} t \qquad (10)$$

Fig. 12 shows the pseudo second order kinetic plot for the adsorption of Pb (II) ions onto I-CS composite. Equilibrium adsorption capacity (q_e) and the pseudo second order rate constant K_2 were obtained from the slope and intercept of the plots of t/q_t against t.

The kinetic parameters such as rate constants, equilibrium adsorption capacities and correlation coefficients for Pb (II) adsorption using pseudo first order and pseudo second order models are summarized in Table 3.

The results presented in table 3 clearly shows the lower correlation coefficient for pseudo first order (R^2 = 0.88). Similarly the value of q_e calculated is lower than q_e observed experimentally and not in agreement with each other indicating a poor fit with pseudo first order kinetic model. Furthermore, this kinetic model does not fit well to the whole range of contact time. It would only be applicable over the initial stage of the adsorption process.[60]

The pseudo second order kinetic model was used to determine whether the rate limiting step during the adsorption process was chemisorptions. This model was more likely to predict the behavior over whole range of contact time. The results presented in table 3 clearly shows that the coefficient of determination for pseudo second order (R^2 = 0.99) is higher than pseudo first order. Moreover, calculated q_e value is closer with observed experimental q_e value suggested that the adsorption phenomenon of Pb (II) by I-CS sorbent follows the pseudo second order kinetics. The confirmation of pseudo second order kinetics indicated that the concentrations of both adsorbate and adsorbent are involved in rate limiting step, which may be a chemical adsorption or chemisorptions, which involved valence forces through sharing or exchange of electrons between the metal ions and the adsorbent.[61]

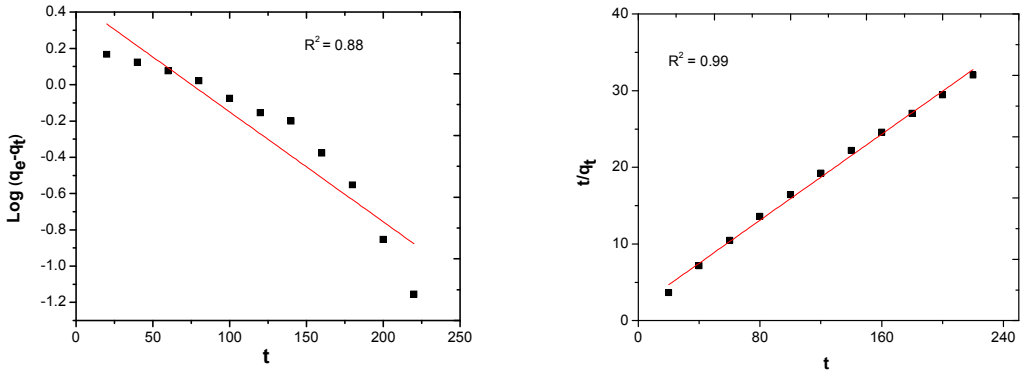

Fig. 12 Plot of t versus Log (q_e-q_t) pseudo first order kinetics and Plot of t versus t/qt pseudo second order kinetics.

3.8 Intraparticle diffusion model

Intraparticle diffusion model is of prime importance because it is rate-determining step in the liquid adsorption systems. During the batch mode of adsorption, there was a possibility of transport of adsorbate into the pores of adsorbent, which is often the rate limiting step. The intraparticle diffusion model developed by Weber and Morris,[62] McKay and Poots.[63] The linear form of equation for intraparticle diffusion is as follows

$$q_t = K_i t^{0.5} + C \qquad (11)$$

Where q_t (mg/g) is the amount of adsorbate adsorbed on the adsorbent surface at particular time t, t is the time of adsorption (min), Ki is the intra-particle diffusion rate constant (mg/g $min^{0.5}$) and C is the intercept which represents the value of the thickness of boundary layer.[64] The intraparticle diffusion plot of q_t against $t^{0.5}$ is shown in Fig. 13. According to this model, the plot of q_t against the square root of time ($t^{0.5}$) should be linear and if these lines passes through the origin then intraparticle diffusion is the rate-controlling step.[65] When the plots do not pass through the origin, this is indicative of some degree of boundary layer control and this further shows that the intraparticle diffusion is not the only rate-limiting step but other kinetic models may also control the rate of adsorption. The intraparticle diffusion parameters K_i and C were obtained from the slope and intercept of plot of q_t versus $t^{0.5}$. The correlation coefficients (R^2 = 0.97) for the intraparticle diffusion model at 27 °C and as the straight line did not pass through the origin indicates that the intra-particle diffusion was the part of the adsorption but not the only rate-controlling step.

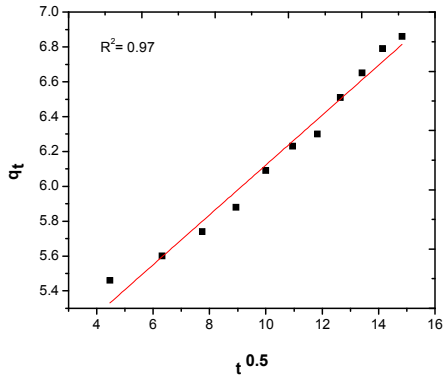

Fig. 13 Plot of square root of time (t) versus q_t intraparticle diffusion model.

Table 3 Adsorption kinetic parameters of pseudo first order, pseudo second order and intraparticle diffusion model.

Metal	Pseudo - first-order			q_e	Pseudo-second-order			Intraparticle diffusion model		
Pb (II)	K_1 (min^{-1})	q_e (mg/g)	R^2	**(cal.)**	K_2 ($g/mg^{-1}min^{-1}$)	q_e (mg/g)	R^2	K_it (mg/g $min^{0.5}$)	C (mg/g)	R^2
Value	0.013	2.851	0.88	6.93	0.010	7.142	0.99	0.143	4.690	0.97

Table 4 Adsorption capacities of Pb (II) ions by various adsorbents.

Adsorbent	q_m (mg/g)	pH	References
chitosan crosslinked with epichlorohydrin-triphosphate	166.94	5	Laus et al. [66]
Chitosan-tripolyphosphate beads	57.33	4.5	Wan Ngah et al. [15]
Graphite doped chitosan composite	6.711	6	Gedam et al. [14]
Epichlorohydrin cross linked chitosan beads	39.42	6	Gyananath and Balhal. [67]
Chitosan	47.393	6	Asandei et al. [68]
Chitosan-immobilized on bentonite	15	4	Futalan et al. [69]
Cross linked chitosan clay beads	7.93	4.5	Tirtom et al. [70]
Bromine pretreated chitosan	1.755	5	Dongre et al. [16]
Iodate doped chitosan composite	22.22	6	This study

The comparative equilibrium adsorption capacity of Pb (II) ions on previously reported adsorbents is given in Table 4. The results revealed I-CS as promising adsorbent as compared to bromine pretreated chitosan for mitigation of Pb (II) from aqueous solution.

4. Conclusions

The present investigation is aimed in the use of I-CS composite as an adsorbent for the removal of heavy metal Pb (II) ions from aqueous solution. The removal of Pb (II) using I-CS sorbent was pH dependent and 95% Pb (II) removal occurred at pH 6 in contact time of 4 hours. Maximum Pb (II) removal efficiency of 98% was achieved at an optimum dose of 0.5 g/L suggested reasonable and cost-effective adsorption technique. The regeneration ability of I-CS adsorbent demonstrated 25-30% decreased percentage recovery of Pb (II) ions at the end of fourth adsorption-desorption cycle.

The adsorption experimental data were fitted to both Langmuir and Freundlich isotherm models with maximum adsorption capacity of 22.22 mg/g obtained from Langmuir isotherm. Adsorption experimental data better obeyed the pseudo second order kinetics model, proposed that the concentrations of both adsorbate and adsorbent are involved in rate-determining step. Adsorption not merely an electrostatic interaction but also involved complexation and ion exchange mechanism.

SEM observations indicated the vital interaction of lead particles at the adsorbent's interface during the adsorption process. The FTIR study revealed the functional groups –OH, C-N, C=O, iodate and NH_2 was concerned with the adsorption performance by I-CS composite. Generally, for pure physisorption process, the adsorptive capacity of sorbent increases with the specific surface area but in this study, the surface area of I-CS adsorbent decreased after modification. In spite of low surface area, the adsorbent found to be effective for Pb (II) removal from aqueous solution. Therefore, it can be concluded that the physisorption of I-CS sorbent for Pb (II) removal is limited and the adsorptive mechanisms will mainly be the chemisorption. The cost of removal of Pb (II) is expected to be quiet low as the adsorbent is economical and easily available in large amount conveys us the new methods and consideration for the increasing pressure of the worldwide environmental pollution.

Acknowledgments

The authors are thankful to Prof. J. S. Meshram for providing their laboratory facilities. Authors are also grateful to the Director, VNIT Nagpur, India for providing technical assistance in the characterization of samples.

References

1. N. Abdus–Salam and F. A. Adekola, The influence of pH and adsorbent concentration on adsorption of lead and zinc on a natural goethite, *African Journal of Science and Technol*., 2005, **6**, 55-66.
2. B. L. Martins, C.C.V. Martins, A.S. Luna and C.A. Henriques, Sorption and desorption of Pb^{2+} ions by dead *Sargassum* sp. biomass, *Biochemical Engineering Journal*, 2006, **27**, 310-314.
3. C. K. Liu, R. B. Bai and Q. S. Ly, Selective removal of copper & lead ions by diethylenetriamine-functionalised adsorbent: behaviors and mechanisms, *Water Research*, 2008, **42**, 1511-1522.
4. V. K. Gupta, M. Gupta and S. Sharma, Process development for the removal of lead and chromium from aqueous solutions using red mud—an aluminium industry waste, *Water Research*, 2001, **35**, 1125–1134.
5. J. H. Qu, Research progress of novel adsorption process in water purification: A review*, J. Environ. Sci.*, 2008, **20**, 1-13.
6. V. K. Gupta and A. Rastogi, Biosorption of Lead (II) from aqueous solutions by non-living algal biomass Oedogonium sp. and Nostoc sp.—a comparative study*, Colloids and Surface B: Biointerfaces*, 2008, **64**, 170–178.
7. V. K. Gupta and I. Ali, Removal of lead and chromium from wastewater using bagasse fly ash—a sugar industry waste *, J. Colloid Interface Sci.,* 2004, **271**, 321–328.

8. S. K. Shrivastava, V.K. Gupta and D. Mohan, Kinetic parameter for the removal of lead and chromium from wastewater using activated carbon developed from fertilizer waste material, *Environmental Modeling & Assessment,* 1996, **1**, 281-290.
9. J. Febrianto, A.N. Kosasih, J. Sunarso, Y. H. Ju, N. Indraswati and S. Ismadji, Equilibrium and kinetic studies in adsorption of heavy metals using biosorbent: A summary of recent studies*, Journal of Hazard. Mat.*, 2009, **162**, 616-645.
10. M. Rinaudo, Chitin and chitosan: Properties and applications*, Prog. Polym. Sci.*, 2006, **31**, 603-632.
11. S. M. Nomanbhay and K. Palanisamy, Removal of heavy metal from industrial wastewater using chitosan coated oil palm shell charcoal*, Electronic J. Biotechnol.*, 2005, **8**, 43–53.
12. N. Sankararamakrishnan and R. Sanghi, Preparation and characterization of a novel xanthated chitosan*, Carbohydrate Polymers*, 2006, **66**, 160-167.
13. L. Fan, C. Luo, M. Sun, X. Li and H. Qiu, Highly selective adsorption of lead ions by water-dispersible magnetic chitosan/graphene oxide composites*, Colloid surf B: Biointerfaces*, 2013, **103**, 523-529.
14. A. H. Gedam, R. S. Dongre and A. K. Bansiwal, Synthesis and characterization of graphite doped chitosan composite for batch adsorption of lead (II) ions from aqueous solution Advanced Materials Letters, 2015, **6**, 59-67.
15. W. S. Wan Ngah and S. Fatinathan, Adsorption characterization of Pb (II) and Cu (II) ions onto chitosan-tripolyphosphate beads: Kinetic, equilibrium and thermodynamic studies*, Journal of Environ. Manag.*, 2010, **91**, 958-969.
16. R. Dongre, M. Thakur, D. Ghugal and J. Meshram, Bromine pretreated chitosan for adsorption of lead (II) from water, *Bulletin of Material Science*, 2012, **35**, 875-884.
17. T. Budnyak, V. Tertykh and E.Yanovska, Chitosan Immobilized on Silica Surface for Wastewater Treatment*, Materials Sci.*, 2014, **20**, 177.
18. M.W. Wan, C.C. Kan, B.D. Rogel and M.L.P. Dalida, Adsorption of copper (II) and lead (II) ions from aqueous solution on chitosan-coated sand *, Carbohydrate Polym.*, 2010, **80**, 891-899.
19. N. Grisdanurak, S. Akewaranugulsiri, C.M. Futalan, W. C. Tsai, C. C. Kan, C. W. Hsu and M. W. Wan, The study of copper adsorption from aqueous solution using cross linked chitosan immobilized on bentonite*, J. Appl. Polym. Sci.*, 2012, **125**, 132-142.
20. A. Zhang, S. Hu, J. Xiang, P. Fu, L. Sun, H. Fei, F. Cao, P. Gao and J. Zhang, Adsorption of Hg^0 from Coal Combustion Flue Gases by Novel Iodine-Modified Bentonite/Chitosan Sorbents , Proceedings of Power and Energy Engineering Conference (APPEEC), 2010, pp. 1-4.
21. P. Zhao, X. Guo and C. Zheng, Removal of elemental mercury by iodine-modified rice husk ash sorbents*, Journal of Environmental Sciences*, 2010, **22**, 1629-1636.

22. C. M. Yang and K. Kaneko, Adsorption Properties of Iodine-Doped Activated Carbon Fiber, *Journal of Colloid and Interface Science*, 2002, **246**, 34–39.
23. R. D. Vidic and D. P. Siler, Vapor-phase elemental mercury adsorption by activated carbon impregnated with chloride and chelating agents, *Carbon*, 2001, **39**, 3-14.
24. E. J. Granite, H. W. Pennline and R. A. Hargis, Novel sorbents for mercury removal from flue gas, Chemistry *Research*, 2000, **39**, 1020-1029.
25. H. C. Zeng, F. Jin and J. Guo, Removal of elemental mercury from coal combustion flue gas by chloride-impregnated activated carbon, *Fuel,* 2004, **83**, 143–146.
26. S.Y. Lee, Y.C. Seo and J. S. Jurng, Removal of Gas Phase Elemental Mercury by Iodine-Chloride Impregnated Activated Carbon, *Atmos. En*V*iron*. 2004, **38**, 4887–4893.
27 Y. Pan and D. Xiong, Friction properties of nano-hydroxyapatite reinforced poly (vinyl alcohol) gel composites as an articular cartilage, *Wear*, 2009, **266**, 699-703.
28. G. Lawrie, I. Keen, B. Drew, A. Chandler-Temple, L. Rintoul, P. Fredericks and L. Grondahl, Interactions between alginate and chitosan biopolymers characterized using FTIR and XPS, *Biomacromolecules*, 2007, **8**, 2533-2541.
29. E. de souza costa-Jr, M. M. Pareira and H. S. Mansur, Properties and biocompatibility of chitosan films modified by blending with PVA and chemically cross linked, *Journal of Material Science: Mater. Med.,* 2009, **20**, 553.
30. Y. J. Yin, K. D. Yao, G. X. Cheng and J. B. Ma, Properties of polyelectrolyte complex films of chitosan and gelatin, *Polymer International*, 1999, **48**, 429-432.
31. S. L. Sun and A. Q. Wang, Adsorption Properties and Mechanism of Cross-Linked Carboxymethyl-Chitosan Resin with Zn (II) as Template Ion, *React. Funct. Polym.,* 2006, **66**, 819–826
32. K. D. Girase, P. Z. Zambare, K.S. Chaudhari and D. K. Sawant, Growth and Characterization of Gel Grown Cobalt Iodate Crystals, *Bulg. J. Phys*. 2014, **41**, 315–320.
33. K. D. Girase, Infrared, Raman spectra and thermal studies of lead iodate crystals doped with Zinc (II), *Journal of Chemical and Pharmaceutical Research*, 2014, **11**, 444-447.
34. K. Nakamoto, Infrared spectra of inorganic and coordination compounds: a guide to FTIR spectra, Wiley, New York, 2nd edn. 1970.
35. P. Ramamurthy and E. A. Secco, Studies on metal hydroxy compounds. XII. Thermal analyses, decomposition kinetics, and infrared spectra of copper basic oxysalts, *Can. J. Chem*., 1970, **48**, 3510-3519.
36. Y. Nuhoglu and E. Malkoc, Thermodynamic and kinetic studies for environmentally friendly Ni(II) biosorption using waste pomace of olive oil factory, *Bioresource Techno*., 2009, **100**, 2375–2380.

37. M. H. M. A. Kamal, W. M. K. W. K. Azira, M. Kasmawati, Z. Haslizaidi and W. N. W. Saime, Sequestration of toxic Pb (II) ions by chemically treated rubber (*Hevea brasiliensis*) leaf powder, *Journal of Environ. Sci.,* 2010, **22**, 248-256.

38. A. M. Farhan, A. H. Al-Dujaili and A. M. Awwad, Equilibrium and kinetic studies of cadmium(II) and lead(II) ions biosorption onto Ficuscarcia leaves, *International Journal of Indus. Chem.,* 2013,**4**, 24.

39. C. Bangyekan, D. Aht-Ong and K. Srikulkit, Preparation and properties evaluation chitosan-coated cassava starch films, Carbohydrate *Polym.*, 2006, **63**, 61-71.

40. J. T. Yeh, C. L. Chen, K. S. Huang, Y. H. Nien, J. L. Chen and P. Z. Huang, Synthesis, characterization and application of PVP/chitosan blended polymers, *J. of Applied Polymer Sci.,* 2006, **101**, 885-891.

41. G. P. Ma, D. Z. Yang, J. F. Kennedy and J. Nie, Synthesize and characterization of organic-soluble acylated chitosan, *Carbohydrate Polym.*, 2009, **75**, 390-394.

42. L. Wang, J. Zhang and A. Wang, Removal of methylene blue from aqueous solution using chitosan-*g*-poly (acrylic acid)/montmorillonite super adsorbent nanocomposite, *Colloids and Surfaces A: Physicochemical and Engineering Aspects*, 2008, **322**, 47-53.

43. I. D. Mall, V. C. Srivastava, G. V. A. Kumar and I. M. Mishra, Characterization and utilization of mesoporous fertilizer plant waste carbon for adsorptive removal of dyes from aqueous solution, *Colloids and Surfaces A – Physicochemical and Engineering Aspects*, 2006, **278**, 175-187.

44. G. V. Tagliaferro, P. H. F. Pereira, L. A. Rodrigues, M. L. C. P. Silva, Cadmium, lead and silver adsorption in hydrous niobium oxide prepared by homogeneous solution method, Quimica Nova, *Química Nova*, 2011, **34**, 101-105.

45. M. Momčilović, M. Purenović, A. Bojić, A. Zarubica, and M. Randelovid, Removal of lead (II) ions from aqueous solutions by adsorption onto pine cone activated carbon, *Desalination*, 2011, **276**, 53–59.

46. S. Doyurum and A. Çelik, Pb (II) and Cd (II) removal from aqueous solutions by olive cake, *Journal of Hazardous Materials*, 2006, **138**, 22–28.

47. S. Tunali, T. Akar, A. S. Özcan, I. Kiran, and A. Özcan, Equilibrium and kinetics of biosorption of lead(II) from aqueous solutions by *Cephalosporium aphidicola, Separation and Purification Technology*, 2006, **47**, 105–112.

48. L. Dong, Z. Zhu, H. Ma, Y. Qiu and J. Zhao, Simultaneous adsorption of lead and cadmium on MnO_2-loaded resin, *Journal of Environmental Sciences*, 2010, **22**, 225–229.

49. N. Prakash, P. N. Sudha and N. G. Renganathan, Copper and cadmium removal from synthetic industrial wastewater using chitosan and nylon 6, *Environ Sci. Pollut Res.*, 2012, **19**, 2930–2941.

50. A. Guenay, E. Arslankaya and I. Tosun, Lead removal from aqueous solution by natural and pretreated clinoptilolite: Adsorption equilibrium and kinetics, *J. Hazard Mater.*, 2007, **146**, 362–371.
51. M. A. Mohd Salleh, D. K. Mahmoud, W. A. Wan Abdul Karim and A. Idris, Cationic and anionic dye adsorption by agricultural solid wastes: a comprehensive review, *Desalination*, 2011, **280**, 1–13.
52. I. Langmuir, The Adsorption of Gases on the Plane Surfaces of Glass, Mica, and Platinum, Journal *of American Chemical Society*, 1918, **40**, 1361-1403.
53. T. W. Weber Jr. and R. K. Chakravorty, Pore and solid diffusion models for fixed-bed adsorbers, J. *Am. Inst. Chem. Eng*, 1974, **20**, 228–238.
54. H. M. F. Freundlich, Over the adsorption in solution, *J. Phys. Chem.*, 1906, **57**, 385-471.
55. H. Chen, Y. Zhao and A. Wang, Removal of Cu (II) from aqueous solution by adsorption onto acid-activated palygorskite, *J. Haz. Materials,* 2007, **149**, 346-354.
56. Y. Bulut and Z. Tez, Removal of heavy metals from aqueous solution by sawdust adsorption *J. of Environmental sciences*, 2007, **19**, 160-166.
57. S. Lagergren, About the theory of so-called adsorption of soluble substances, *Hand linger*, 1898, **24**, 1-39.
58. Y. S. Ho, Review of Second-Order Models for Adsorption Systems, *J. Hazard Mater*, 2006, **136**, 681–689.
59. Y. S. Ho and G. McKay, Sorption of Dye from Aqueous Solution by Peat, *Chem. Eng. J.*, 1998, **70**, 115–124.
60. G. Crini and P.M. Badot, Application of chitosan, a natural amino polysaccharide, for dye removal from aqueous solutions by adsorption processes using batch studies: A review of recent literature, *Prog. Polym. Sci*., 2008, **33**, 399-447.
61. M. Hasan, A. L. Ahmad and B. H. Hameed, Adsorption of reactive dye onto cross-linked chitosan/oil palm ash composite beads, *Chem. Eng. J*., 2008, **136**, 164-172.
62. W. J. Weber and J. C. Morris, Advances in water pollution research: removal of biologically resistant pollutants from waste waters by adsorption, Proceedings of International Conference on Water Pollution Symposium, Pergamon Press, Oxford, 1962, pp. 231-266.
63. G. McKay and V. J. P. Poots, Kinetics and diffusion processes in colour removal from effluent using wood as an adsorbent, *J. Chem. Technol. & Biotechnol*., 1980, **30**, 279-292.
64. A. T. Mohd Din, B. H. Hameed and A. L. Ahmad, Batch adsorption of phenol onto Physiochemical-activated coconut shell, *J. Hazard. Mater.,* 2009, **161**, 1522–1529.
65. Y. P. Teoh, M. A. Khan and T. S. Y. Choong, Kinetic and isotherm studies for lead adsorption from aqueous phase on carbon coated monolith, *Chemical Engineering Journal*, 2013, **217**, 248–255.

66. R. Laus, T.G. Costa, B. Szpoganicz and V.T. Favere, Adsorption and desorption of Cu(II), Cd(II) and Pb(II) ions using chitosan cross linked with epichlorohydrin-triphosphate as the adsorbent, *J. Haz. Mater*., 2010, **183**, 233-241.

67. G. Gyananath and D. K. Balhal, Removal of lead (II) from aqueous solutions by adsorption onto chitosan beads, *Cellulose Chem. Technol*., 2012, **46**, 121-124.

68. D. Asandei, L. Bulgariu and E. Bobu, Lead (II) removal from aqueous solutions by adsorption onto chitosan, *Cellulose Chem. Technol*., 2009, **43**, 211-216.

69. C. M. Futalan, W.C. Tsai, S.S. Lin and K.J. Hsien, Copper, nickel and lead adsorption from aqueous solution using chitosan-immobilized on bentonite in a ternary system, *Sustain. Environ. Res*., 2012, **22**, 345-355.

70. V. N. Tirtom, A. Dincer, S. Becerik, T. Aydemir and A. Celik, Removal of lead (II) ions from aqueous solution by using cross linked chitosan-clay beads, *Desalination and water treatment,* 2012, **39**, 76-82.